Feasibility of a Cochlear Nucleus Auditory Prosthesis Based on Microstimulation

Contract No. NO1-DC-8-2102

QUARTERLY PROGRESS REPORT #5

July 1-September 30, 1999

HUNTINGTON MEDICAL RESEARCH INSTITUTES
Neurological Research Laboratory
734 Fairmont Avenue
Pasadena, California 91105

DB McCreery, PhD
TGH Yuen, PhD
LA Bullara, BS
WF Agnew, PhD

HOUSE EAR INSTITUTE
Department of Neuroanatomy and
Department of Auditory Implants and Prostheses
2100 West Third Street
Los Angeles, California 90057

JK Moore, PhD
RV Shannon, PhD
S Otto, BS

Design of the Microstimulation Electrode Array

Section D of the work statement charges House Ear Institute with preparing for microstimulation of the ventral cochlear nucleus of a deaf human by determining optimal design of the electrode array. Design specification should include the number, size, spacing and orientation of the stimulating electrodes. We have approached this project by carrying out interactive modeling of the human ventral cochlear nucleus and the proposed electrode in AutoCAD three-dimensional reconstructions.

As in previous contracts, our modeling of the human cochlear nuclei and surrounding structures has been based on human postmortem material obtained through the donor program of the Temporal Bone Bank at House Ear Institute. Donated brainstems of former House Ear Clinic patients received in our laboratory are embedded in celloidin, sectioned at 75 μm, and stained for cells (Nissl stain) and myelinated fibers (Woelcke stain). From a series of every 8th section, enlarged drawings are made of one half of the brainstem, and these drawings are digitized into the Jandel PC3D program (methods described in final report of 1989-1992 contract). Fig. 1 is an illustration of a PC3D wireframe reconstruction of the cochlear nuclear complex and surrounding brainstem structures. In this figure, auditory structures (shown in red) include the dorsal cochlear nucleus (DCN), ventral cochlear nucleus (VCN), axons of the trapezoid body (TB) extending from the VCN into the brainstem, and the superior olivary complex (SOC). Nonauditory structures include the vestibular nuclei (VN, shown in green), the spinothalamic tract (STT, shown in yellow), and the facial nucleus and nerve (VII, VIIn, shown in blue). The cochlear nuclei curve around the lateral edge of the inferior cerebellar peduncle (ICP), a collection of axons passing from the spinal cord and brainstem to the cerebellum. The cochlear and vestibular divisions of the eighth nerve (VIIIn) run beneath the VCN to enter the brainstem along the medial surface of the nucleus. Finally, on the lateral surface of the cochlear nuclei, the lateral recess (LR) forms sleeve-like extension of the fourth ventricle through which cerebrospinal fluid passes into the subdural space. PC3D files such as this were transferred into the AutoCAD program in order to create solid-surface models of anatomical structure and carry out interactive modeling with various types of microelectrode arrays (methods described in final report of 1992-95 contract).

Our early contract investigations of the shape and volume of the human cochlear nuclei in subjects with various pathologies demonstrated that some degree of flattening of the cochlear nuclei occurs in subjects with acoustic neuromas caused by neurofibromatosis (Fig. 2). For this reason, the present

study was based on reconstruction of the brainstem of a patient with two large bilateral tumors. The tumors had been removed 10 and 7 years, respectively, before the patients death, and a surface ABI device had been implanted in the lateral recess at the time of the second tumor surgery.

The target of microstimulation is the ventral cochlear nucleus. This assumption is based on a body of work in animals which indicates that the dorsal cochlear nucleus does not form the primary perceptual pathway for auditory stimuli. Thus in the present study, we have included only the modules for the VCN and the brain surface. Figure 3 presents a view of the ventral cochlear nucleus (shown in red) from the posterior (inferior) and medial aspect of the nucleus, and thus gives a view of the posterior ventral cochlear nucleus (PVCN). Dashed lines indicate the direction of the tonotopic planes of the nucleus, which run upward at about a 45° angle from the point of bifurcation of eighth nerve axons within the nerveroot (based on Moore and Osen, 1979). On the outer (lateral) surface of the nucleus is the lateral recess. The taenia choroidea (shown in green) is a ridge at the mouth of the recess where the ependymal lining of the recess meets the outer pial surface of the brainstem. The juxtaposition of the shiny ependymal surface with the dull pial surface makes this a visible landmark for the neurosurgeon, one that is currently used to aid in placement of the surface electrode array within the lateral recess.

To determine the depth of penetration of the electrodes into the VCN, it is necessary to view the nucleus from a different perspective. Figure 4 illustrates a view of the ventral cochlear nucleus (shown in red) in the horizontal plane. The triangular extension on the medial side of the nucleus is the nerve root, which in a normal-hearing subject is the point of entry of axons of the cochlear nerve, but in a post-surgical tumor patient would contain only gliotic scar tissue replacing degenerated axons. The nerve root would thus not be part of the target for the microelectrodes. Dashed lines indicate the normal course of cochlear axons entering the anterior and posterior portions of the ventral nucleus (AVCN, PVCN). We assume that the frequency-specific organization of VCN neurons remains, at least to some degree, after degeneration of cochlear nerve axons. Two other portions of the VCN are also not ideal locations for microelectrode implantation. As discussed in QPR #1 of the present contract (October, 1998), the spherical cell area at the rostral tip of the VCN contains neurons which project to nuclei in the superior olivary complex (Warr, 1982; Cant and Casseday, 1986) and are responsible for integration of binaural input. In an animal experiment conducted last year at HMRI, microstimulation to this area did not produce excitation at the level of the inferior colliculus. Thus we would not target the rostral tip for microstimulation. On the lateral side of the nucleus, the cap area contains predominantly small GABAergic and glycinergic inhibitory interneurons, rather

than neurons projecting to higher levels of the brainstem (Moore et al., 1996). Presumably stimulation here would not evoke conscious perception of auditory stimuli. The preferred target area is thus the central and posterior VCN, which is composed mainly of neurons projecting directly to the contralateral inferior colliculus (Adams, 1979; Brunso-Bechtold et al., 1981).

This reconstruction shown in Figure 4 also includes some indication of the location of structures surrounding the VCN. The anterior half of the human VCN lies buried in the middle cerebellar peduncle and is not directly accessible to microstimulation. Medial to the PVCN is the inferior cerebellar peduncle which is, as previously noted, a large collection of myelinated axons carrying information to the cerebellum. Laterally, the position of the brainstem surface is indicated by the taenia choroidea (shown in yellow), which is the surface landmark to be used for placement of the penetrating electrode array. It is separated from the PVCN by a layer of glial processes and endfeet approximately 0.5 mm wide. The geometry of the structures surrounding the VCN has clarified an observation which has puzzled us, namely, that tumor cases show a flattening of the PVCN, but not the AVCN, compared to nontumor patients. We now believe this is due to compression of the posterior half of the VCN between the enlarging tumor mass in the cerebellopontine angle and the relatively incompressible inferior cerebellar peduncle.

Our first estimate of the appropriate design for the microelectrode array is shown in Figure 5. This shows the four activated iridium stimulating electrodes with lengths of 1.5, 2.0, 2.5 and 3.0 mm. The ball tips were added to the computer model to insure that we could visualize the stimulation sites at the tips of the electrode wires. The individual wire electrodes are held in an epoxy disk base which is 2.0 mm in diameter. The actual design also includes two inactive stabilizing pins, each 4 mm in length, but these inactive pins were omitted from this model so as not obscure the location of the tips of the stimulating electrodes.

Based on the reconstruction shown in Figure 4, our estimate of the target area for implantation is a rectangular volume of VCN tissue, approximately 2 mm in the oblique anterioposterior dimension and 1 mm in the mediolateral dimension. This block of tissue is superficial only posteriorly, where it is separated from the brainstem surface by a half millimeter of glial tissue. Modeling of insertion of the electrode array into the VCN is shown in Figure 6. This is one of a number of tilts, angles and rotations at which the insertion was simulated. In each case, we separated the epoxy disk of the electrode array from the actual brain surface by a distance of 0.5 mm in order to allow for the connective tissue capsule that will form around the electrode base after implantation. In all simulated insertions, the tip of the electrode wire 3 mm in

length was located medial to the VCN. In every case, however, the tips of the 1.5, 2.0 and 2.5 mm electrode wires were located within the VCN. Based on these results, we plan to fabricate an electrode array with six stimulating electrodes with lengths of 1.5, 1.5, 2.0, 2.0, 2.5 and 2.5 mm (Fig. 7). The array will also include two inactive stabilizing pins 3.0 mm in length. We believe that this design will maximize the chances of placing the stimulating sites within the body of the VCN. The 45° tilt of the tonotopic planes should insure that tips of equivalent length will lie in different planes of the nucleus.

References

Adams JC (1979) Ascending projections to the inferior colliculus. J Comp Neurol 183:519-538.

Brunso-Bechtold JK, Thompson GC and Masterton RB (1981) HRP study of the organization of auditory afferents asending to central nucleus of the inferior colliculus in cat. J Comp Neurol 197:705-722.

Cant NB and Casseday JH (1986) Projections from the anteroventral cochlear nucleus to the lateral and medial superior olivary nuclei. J Comp Neurol 247:447-476.

Moore JK and Osen KK (1979) The cochlear nuclei in man. Am J Anat 154:393-418.

Moore JK, Osen KK, Storm-Mathisen J and Ottersen OP (1996) Gamma-aminobutyric acid and glycine in the baboon cochlear nuclei: an immunocytochemical colocalization study with reference to interspecies differences in inhibitory systems. J Comp Neurol 369: 497-519.

Warr WB (1982) Parallel ascending pathways from the cochlear nucleus: neuroanatomical evidence of functional specialization. Contrib Sens Physiol 7:1-38.

Fig. 1

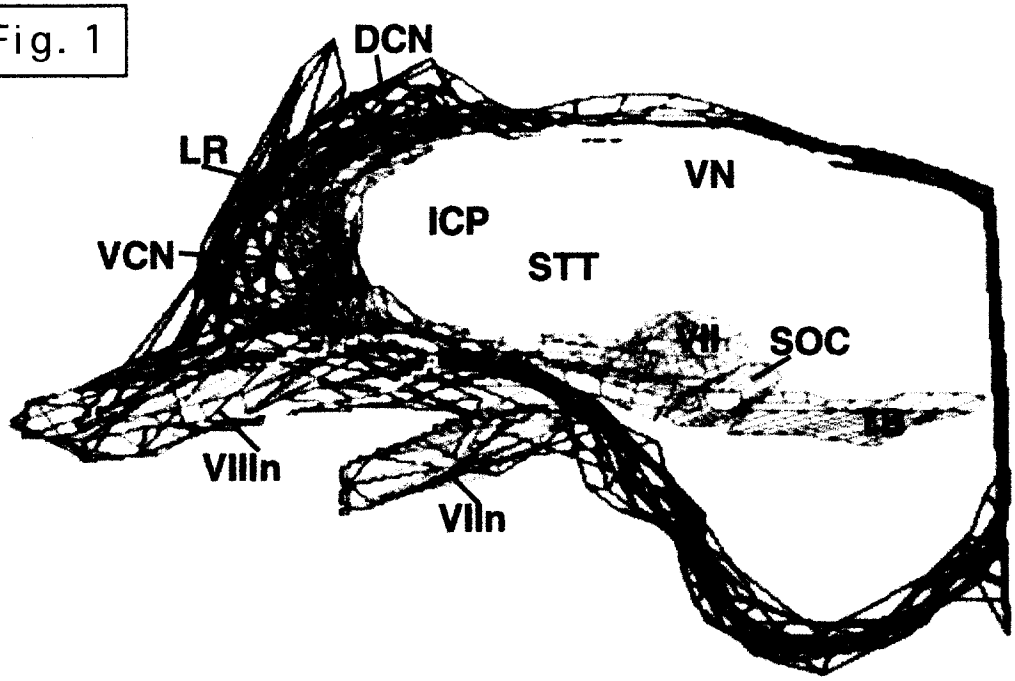

Fig. 2

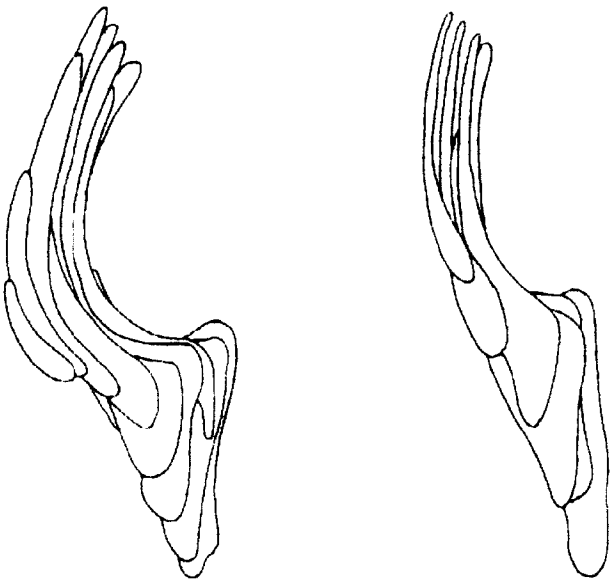

H90-35
Normal

H89-54
Acoustic neuroma

Fig. 3.

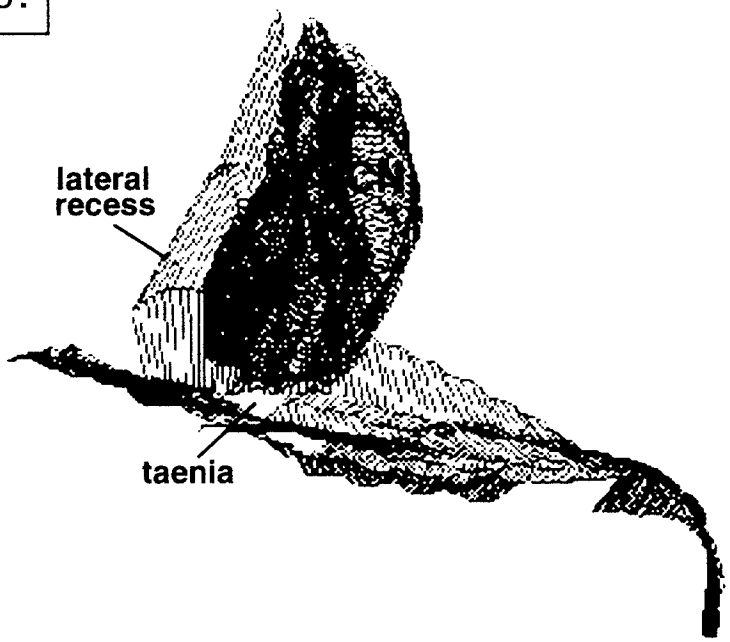
lateral
recess
taenia

Fig. 4

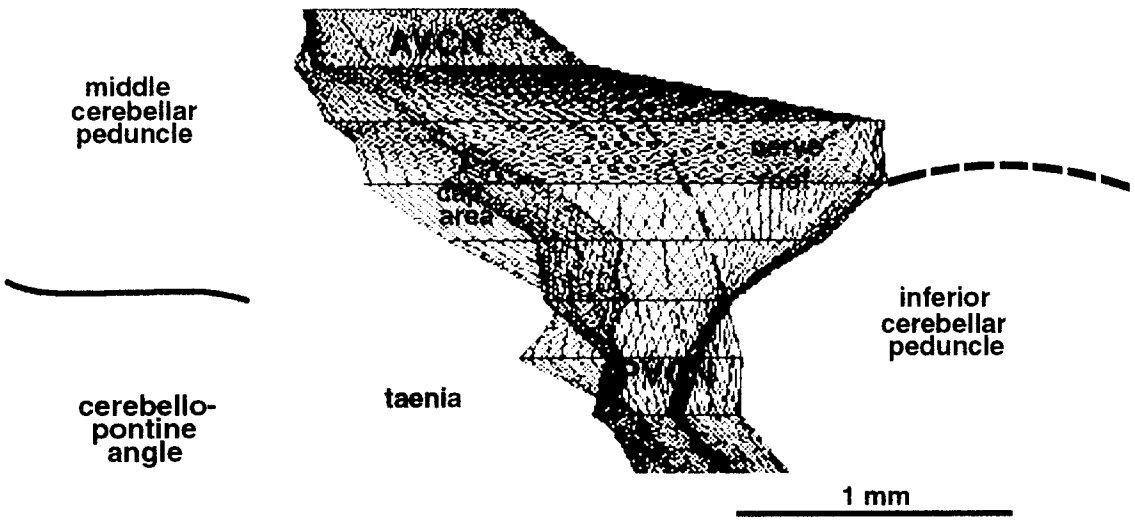
middle
cerebellar
peduncle
AVCN
nerve
root
dark
area
inferior
cerebellar
peduncle
cerebello-
pontine
angle
taenia
1 mm

Fig. 5

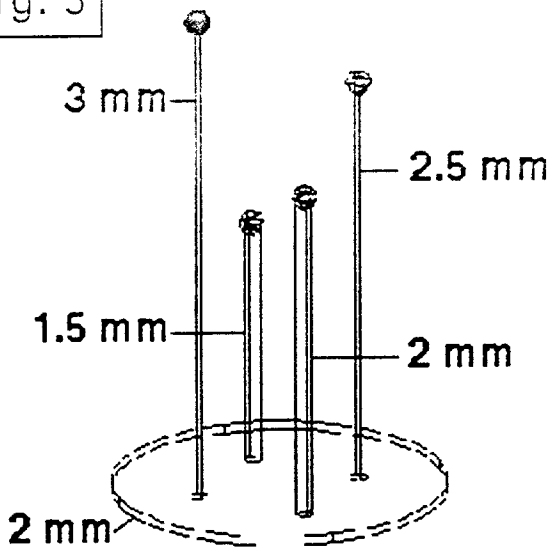

Fig. 6

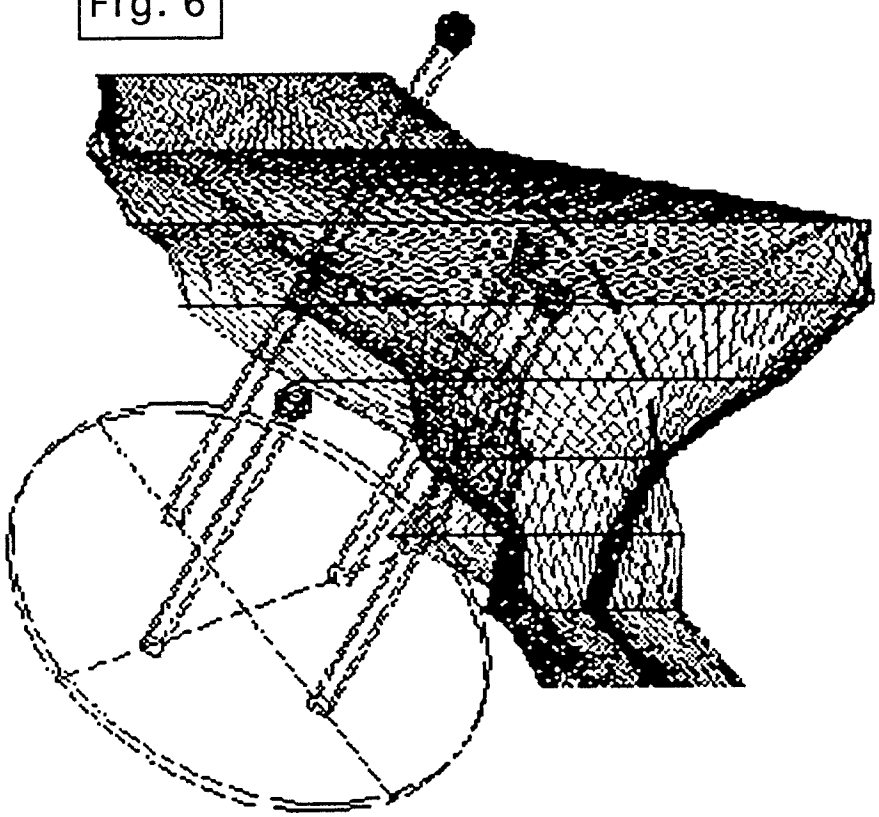

Fig. 7